



## Fragmentation of phosphorylated and singly charged peptide ions via interaction with metastable atoms

Vadym D. Berkout\*, Vladimir M. Doroshenko

MassTech, Inc., 6992 Columbia Gateway Dr., Columbia, MD 21046, United States

### ARTICLE INFO

#### Article history:

Received 28 December 2007  
Received in revised form 24 April 2008  
Accepted 25 April 2008  
Available online 3 May 2008

#### Keywords:

Time-of-flight  
Fragmentation  
Phosphorylation  
Metastable atom

### ABSTRACT

Fragmentation of phosphorylated peptide ions via interaction with electronically excited metastable argon atoms was studied in a linear trap–time-of-flight mass spectrometer. Doubly charged ions of phosphorylated peptides from an Enolase digest were produced by electrospray ionization and subjected to a metastable atom beam in the linear trap. The metastable argon atoms were generated using a glow-discharge source. An intensive series of c- and z-ions were observed in all cases, with the phosphorylation group intact. The formation of molecular radical cations with reduced charge indicated that an electron transfer from a highly excited metastable state of argon to the peptide cation occurred. Additionally, singly charged Bradykinin, Substance P and Fibrinopeptide A molecular ions were fragmented via interaction with electronically excited metastable helium atoms. The fragmentation mechanism was different in this case and involved Penning ionization.

© 2008 Elsevier B.V. All rights reserved.

### 1. Introduction

Mass spectrometry (MS) is now widely used in protein biochemistry and in proteomics for the identification and characterization of proteins [1]. Collision induced dissociation (CID) is the most commonly used approach to derive structural information from peptide and protein ions through collisions with neutral gas molecules [2]. In this process, which generally leads to cleavage of the peptide backbone amide bond to produce b-type and y-type sequence ions, peptides are kinetically excited and undergo multiple collisions with neutral gas molecules. Energy acquired in each collision is rapidly distributed throughout all covalent bonds. Fragment ions are formed when the internal energy exceeds the activation barrier required for a particular bond cleavage. The drawbacks of CID include the facile losses of labile groups involved in many important posttranslational modifications, such as phosphorylation and glycosylation, and in many cases incomplete backbone fragmentation [3]. Therefore, developing alternative peptide fragmentation methods is of a considerable interest.

McLafferty and co-workers introduced a new technique, called electron capture dissociation (ECD), which has been shown to complement the information obtained with CID of multiply protonated peptide cations [4]. Capture of a thermal electron by a protonated peptide is exothermic by  $\approx 6$  eV and causes frag-

mentation of N–C $_{\alpha}$  bonds, yielding N-terminal c- and C-terminal z-fragments [5,6]. In contrast to collision-induced dissociation, ECD is believed to be non-ergodic [4], i.e., the cleavage happens prior to any intramolecular energy redistribution. As a result, labile modification groups are preserved. ECD generally results in cleavage of a wider range of peptide backbone bonds than CID with less dependence on peptide composition [7]. However, to this day ECD has only been successfully realized in FT-ICR mass spectrometers, where the electric field is very weak and the strong magnetic field confines electrons. The presence of strong (100–1000 V of amplitude) radio frequency (RF) electric fields in 3D and linear quadrupole ion traps hampers the introduction of low energy electrons to the area where ions are located. Recent attempts to implement ECD into radiofrequency ion traps revealed diminished fragmentation efficiency and sensitivity (as compared to FT-ICR) [8,9].

A new fragmentation technique—electron transfer dissociation (ETD), overcoming the technical challenges of introducing low energy electrons into strong oscillating RF fields, was recently proposed [10–12]. In ETD a singly charged anion transfer an electron to the multiply protonated peptide and induces fragmentation of the peptide backbone along pathways that are similar to those observed in electron capture dissociation. Simultaneous trapping of cations and anions is readily accomplished by the RF quadrupole field. However, it has been noted, that the peptide structural information that can be obtained using ETD is charge-state dependent [13]. The doubly-charged peptide cations give much poorer sequence coverage, than triply protonated cations, with fragmentation often

\* Corresponding author. Tel.: +1 443 539 1701.

E-mail address: [vberkout@apmaldi.com](mailto:vberkout@apmaldi.com) (V.D. Berkout).

limited to one or both ends of the peptide. It was also demonstrated that the efficiency of electron transfer dissociation decreases with peptide size [14].

Another recently introduced fragmentation technique, similar to ECD, is based on the electron transfer from metastable, electronically excited atoms [15,16]. The peptide cations are stored in the RF ion trap and irradiated by a beam of particles generated by a fast atom bombardment (FAB) gun [15] or by a beam of metastable atoms produced in a glow discharge [16]. Since the beam is neutral, problems inherent to the charge capacity limitations of ion traps are not encountered. Fragmentation spectra of common peptides were similar to the spectra observed using ECD [16]. In this study we present further development of this fragmentation technique for analysis of phosphorylated peptides and singly charged peptide ions (which cannot be fragmented using ECD/ETD techniques).

## 2. Experimental

### 2.1. Reagents

Solutions of peptides were prepared in molecular biology grade water (Cambrex Bio Science, Rockland, ME), reagent grade methanol, and glacial acetic acid (Sigma–Aldrich, St. Louis, MO) (1% in 1/1 water/methanol). Substance P, Bradykinin and Fibrinopeptide A were purchased from Sigma–Aldrich (St. Louis, MO). Phosphopeptide standard was purchased from Waters (Milford, MA) and was used without further purification. Helium (ultra high purity grade) and argon (research grade) were supplied by Airgas (Radnor, PA).

### 2.2. Mass spectrometry

The time-of-flight mass spectrometer with orthogonal acceleration used in the present study has been described previously [16]. The schematic illustration of the instrument is shown in Fig. 1. Ions were produced in an electrospray source and transferred into the

mass spectrometer through an atmospheric pressure (AP) interface. The AP interface consists of a heated capillary (0.4 mm i.d.) and a quadrupole ion guide (6.35-mm rod diameter) operated at  $\sim 1$  Torr pressure in the RF-only mode.

The octopole ion guide (3.2 mm rod diameter), located after the quadrupole, was differentially pumped by a small turbomolecular pump to a pressure of  $\sim 0.1$  Torr. Both the quadrupole and octopole were driven by an RF generator, built in-house, according to the design described in Ref. [17]. A capacitive divider allowed the application of different RF amplitudes to the quadrupole and octopole ion guides, respectively. The quadrupole and octopole rods were offset to DC potential, applied through decoupling capacitors.

In contrast to the instrument described earlier [16], a mass resolving quadrupole was placed in a separate differentially pumped chamber. This allowed operating it at pressures of  $\sim 10^{-5}$  Torr in typical experimental conditions, thus providing better precursor selection in comparison with the previous design where it operated at a few mTorr. In the initial experiments the mass resolving quadrupole was driven by a SRS (Sunnyvale, CA) Model DS340 sine-wave signal generator coupled through an ENI (Rochester, NY) Model 240L broadband RF power amplifier. An RF coupling transformer, built in-house, gave an output voltage 0–500  $V_{0-p}$  (zero-to-peak and pole to ground voltage) in the frequency range of 100 kHz to 5 MHz. The transformer also provided the required  $180^\circ$  phase difference between the rod pairs. Later, the mass resolving quadrupole was driven by an Extrel (Pittsburgh, PA) Model 150-QC RF/DC power supply, which provided better precursor ion mass selection.

The last quadrupole was operated in a trapping mode. The DC voltages, applied to the entrance and exit apertures of the last quadrupole, were changed by NAND gate integrated circuitry SN74LS03 with open collector outputs (Texas Instruments, Dallas, TX) controlled by SRS (Sunnyvale, CA) Model DG535 digital signal generator. A beam of metastable electronically excited argon atoms was produced in a glow-discharge source and introduced between the quadrupole rods. The glow-discharge source used in the present study has been described previously [16]. One of its

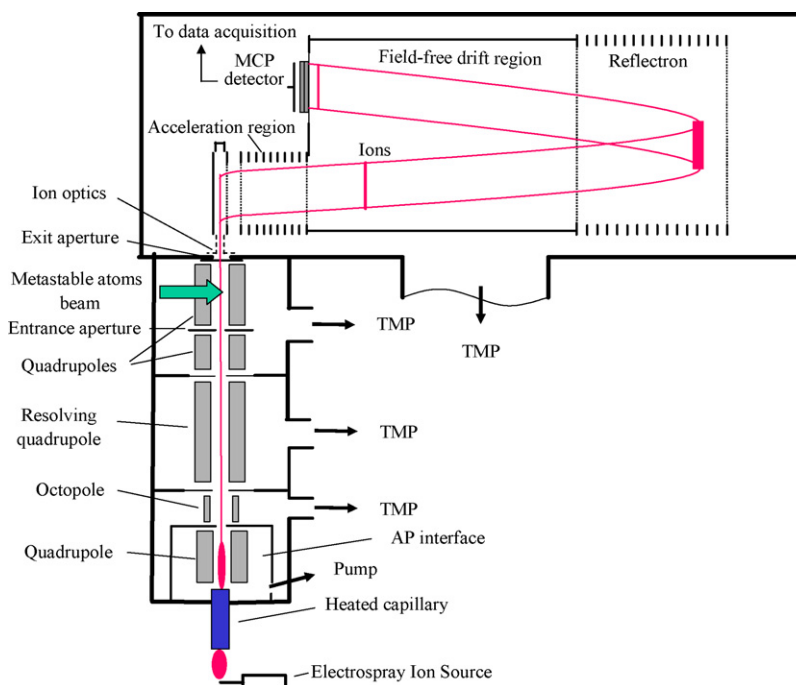


Fig. 1. Schematic view of an ortho-TOF mass spectrometer.

features is an asymmetrical electric field between a radially separated cathode and anode. The asymmetrical field allows better separation of the neutral metastable atoms and the charged particles. A tapered rod (1.5 mm dia.) made from oxygen free copper, located in the high-pressure discharge chamber, serves as the cathode. The anode is planar and is located off-axis immediately after the aperture separating the discharge and quadrupole chambers. The use of a planar electrode for the anode increases stability of the discharge (by providing a larger surface to collect electrons). The discharge ( $I \approx 2\text{--}10\text{ mA}$ ,  $V \approx 300\text{ V}$ ) was initiated by applying high voltage through a limiting  $1.0\text{ M}\Omega$  resistor. A negative potential was applied to the cathode, while the anode was grounded. The high-pressure chamber has a 0.5 mm dia. exit aperture. The pressure in the discharge chamber (where the cathode is located) was 10–25 Torr, while the pressure in the quadrupole region was 5–10 mTorr. Two lenses, located downstream, are covered by nickel grids (BuckbeeMears, St. Paul, MN). To prevent penetration of any remaining electrons into the quadrupole region, the lenses were held at a few hundred volts of negative potential. The gas, supplied to the source (argon or helium), created an expanding flow which carried metastable atoms into the quadrupole ion guide. This low kinetic energy beam of metastable atoms interacted with peptide ions collimated along the central axis of the quadrupole ion guide, causing their fragmentation.

After ejection from the linear quadrupole ion trap the ions were focused by an Einzel lens into the pulser region of the time-of-flight mass analyzer. The time-of-flight analyzer chamber was pumped down by two Leybold (Export, PA) Model Turbovac 361 3501/s turbomolecular pumps to a pressure of the order of  $10^{-7}$  Torr. Deflection plates shield the low energy ion beam from the high voltages applied to the accelerator column, and also make a final adjustment of the beam. Initially, the electric field in the gap of the pulser region is negligible. The last grid of the extraction plates is held at a small positive potential (typically 6–12 V) to prevent field penetration [18] from the accelerator column into the pulser region. When the pulser region is filled with ions, both push-out and draw-out voltage pulses are applied simultaneously to the extraction plates. The intermediate plate is kept at ground potential. The extraction pulses, produced by Behlke (Kronberg, Germany) Model HTS 31GSM high voltage push-pull switches, have typical amplitudes of about 460 V, a rise time of 30 ns, and duration of 3  $\mu\text{s}$ . The duration of the pulse is chosen to guarantee that the heaviest ions have enough time to leave the pulser region. After leaving the pulser region, ions are accelerated to energies of about 7 keV by a uniform DC field in the acceleration column. The ions then move with constant velocities in the field free drift region. The lengths of the pulser, acceleration and field free regions are 0.9, 4.6 and 48 cm, respectively. In order to keep the ion source and ion pulser potentials close to the ground, the drift region is floated at a high voltage potential. A perforated metal cover prevents penetration of the ground potential of the vacuum chamber into the drift region, while allowing effective pumping of the inner volume. Having traversed the drift region, ions enter a single-stage electrostatic mirror, which was tuned together with a dual-stage accelerator to provide a second-order space focusing on the initial ion position [19,20]. The field free region is separated from the accelerator column and the electrostatic mirror by BuckbeeMears (St. Paul, MN) grids with 114 wires/in. having a transmission of 88.6%.

The reflected ions pass back through the drift region before striking a detector. The detector was assembled using a Hamamatsu (Bridgewater, NJ) resistance matched pair of microchannel plates (12  $\mu\text{m}$  channel diameter, 12° bias angle). The front plate of the detector was maintained at the same potential as the drift region (–7 kV). The data acquisition system was decoupled from the high voltage on the detector anode by a ferrite transformer. The signal

was amplified by an ORTEC (Oak Ridge, TN) Model 9326 1-GHz amplifier and recorded by a digital signal averager (ORTEC Model FastFlight-2). Voltages for the pulsers, drift region and ion mirror were provided by Applied Kilovolts (Sussex, UK) Models HP10 and HP5 stable, low noise, high voltage power supplies.

### 3. Results and discussion

#### 3.1. Interaction of metastable atoms with different gases

To prove that the above described source generates substantially neutral gas flow with the electronically excited metastable atoms, the entrance capillary was closed and different gases (nitrogen, ammonia) were supplied into the resolving quadrupole section. This created a gas flow along the quadrupoles axis. The resulting pressure in the section of the vacuum chamber, where the quadrupole linear trap and the discharge source are located, was about 0.2 mTorr (background pressure in this section was less than  $2 \times 10^{-6}$  Torr).

The frequency and amplitude of the RF voltage applied to the quadrupole ion guide was tuned to transmit low  $m/z$  ions. Spectra, averaged over 10 s, are shown in Fig. 2.

The energies of the two most populated metastable states  $^3\text{P}_0$  and  $^3\text{P}_2$  of Ar are equal to 11.72 and 11.55 eV, respectively [21]. The energies of the two most populated metastable states  $^1\text{S}_2$  and  $^3\text{S}_1$  of He are equal to 20.61 and 19.82 eV, respectively [21]. The ionization potentials of nitrogen and ammonia are equal to 15.58 eV, and

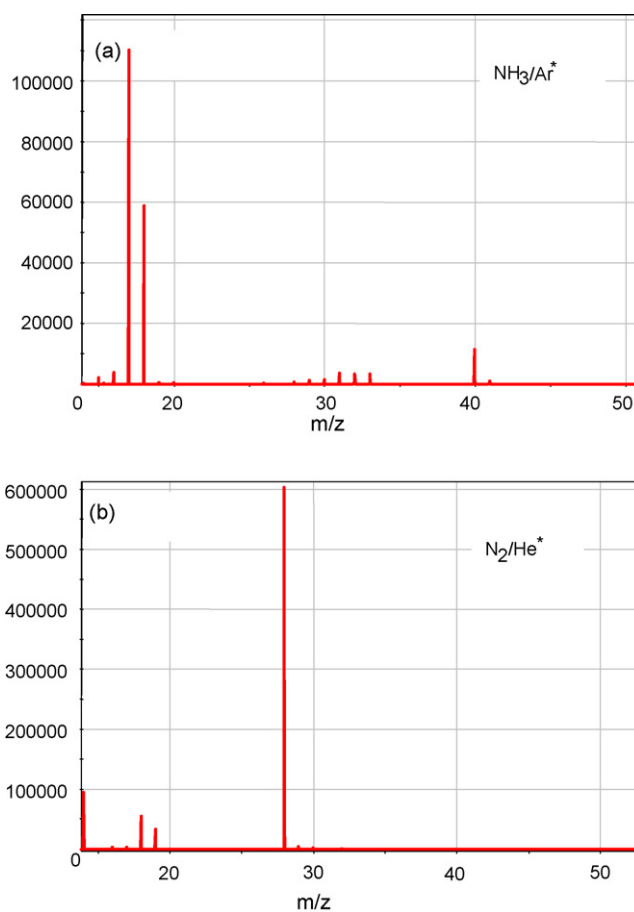
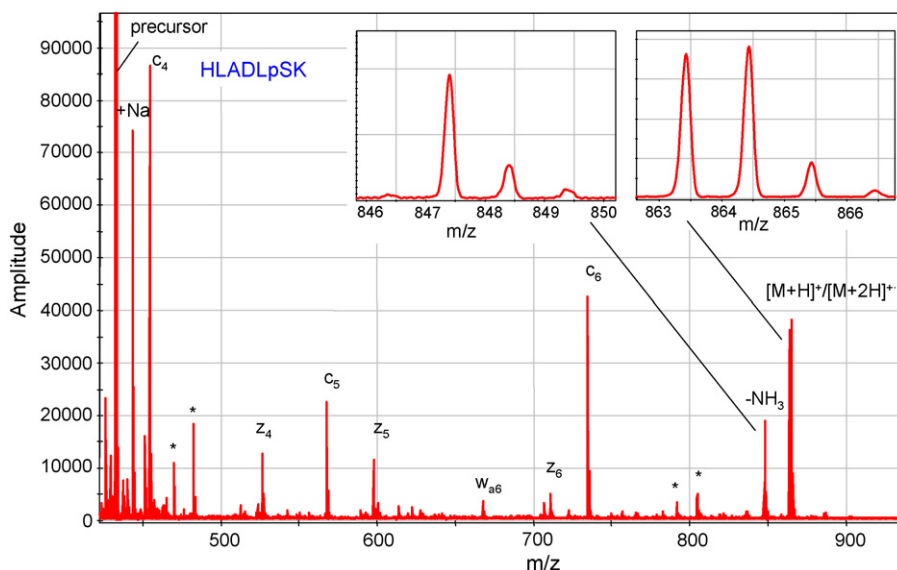


Fig. 2. Ionization spectra of ammonia produced in interaction with metastable electronically excited argon atoms (a) and nitrogen with electronically excited helium atoms (b).



**Fig. 3.** Fragmentation spectrum of doubly charged phosphorylated T19 peptide from an Enolase digest obtained via interaction with metastable argon atoms (\* denotes unassigned peaks).

10.07 eV, respectively [21]. The ionization potential of nitrogen is higher than the energy of the argon metastable levels. No ionization of nitrogen was observed with argon flowing through the discharge source (data not shown). The ionization potential of ammonia is about 1.5 eV lower than the argon  $^3P_0$  and  $^3P_2$  metastable levels. A strong molecular radical cation, produced via Penning ionization, was recorded when ammonia was supplied (Fig. 2a). The energy of the helium metastable states is greater than the nitrogen ionization potential. A strong  $N_2^+$  and  $N^+$  signal was observed when helium was flowing through the discharge source (Fig. 2b). This indicates that the beam entering the quadrupole ion guide consists mainly of neutral particles and contains substantial amounts of metastable electronically excited atoms. Small amounts of argon or helium ions, initially present in the beam, are ejected from the quadrupole ion guide in peptide fragmentation experiments due to a low  $m/z$  cut-off set to  $m/z \sim 250$  in these experiments.

### 3.2. Fragmentation of phosphorylated peptides

Peptide ions were trapped in the last quadrupole for 200 ms to increase the interaction time with metastable, electronically excited argon beam. A mixture of  $5 \mu\text{M}$  phosphorylated peptides from Enolase digest was supplied at a flow rate of  $0.5 \mu\text{l}/\text{min}$  into the electrospray ion source. A doubly charged molecular ion was selected in the mass resolving quadrupole. A home made RF/DC power supply was used in the following experiments, which did not provide a steep cutoff from the heavier mass side. Injection time into the quadrupole linear trap was 2–5 ms. Argon gas was flowing through the source during the experiments and the presence of metastable electronically excited atoms in the argon beam was controlled by turning the discharge on and off. Typically, data were acquired for 30 s. The spectrum of the T19 peptide (phosphorylated at serine), fragmented in interaction

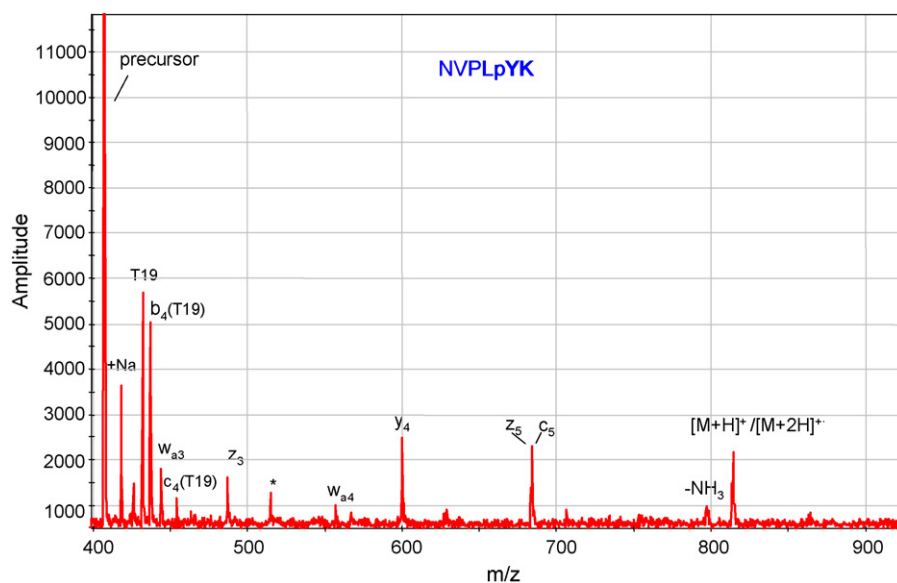


**Fig. 4.** Fragmentation spectrum of doubly charged phosphorylated T18 peptide from an Enolase digest obtained via interaction with metastable argon atoms (\* denotes unassigned peaks).

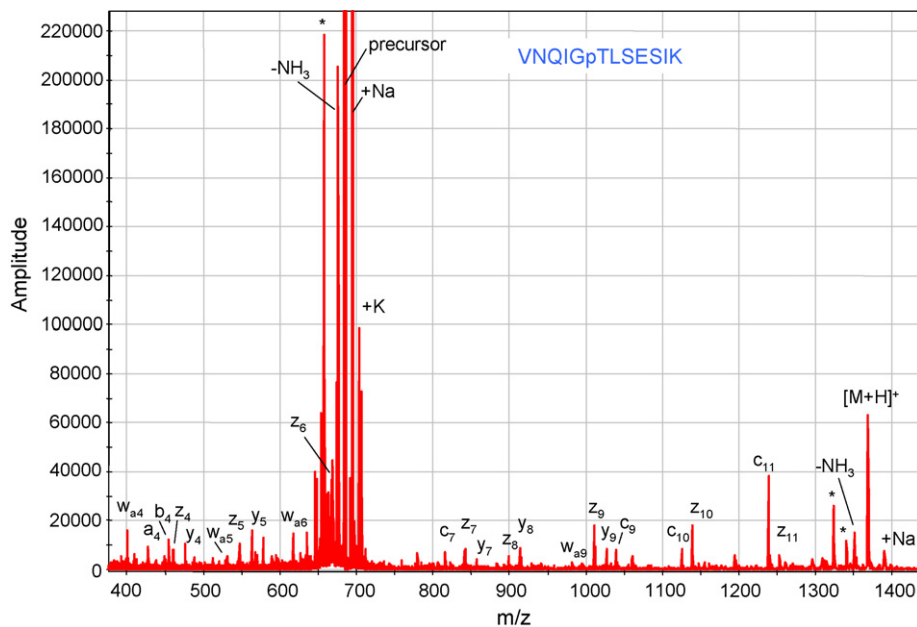


**Fig. 5.** Fragmentation spectrum of doubly charged phosphorylated T43 peptide (VNQIGpTLSESIK) from an Enolase digest obtained via interaction with metastable argon atoms (\* denotes unassigned peaks).

with a low kinetic energy metastable argon beam, is shown in Fig. 3.

The spectrum contains a complete series of c- and z-type ( $z^*$  according to Biemann nomenclature) fragment ions for the recorded mass range. No loss of the phosphate group or phosphoric acid from molecular ion or fragment ions was observed. Ion signals at  $m/z = 469.5(2+)$ , 482.2, 791.3, 804.3 have not been identified. The isotopic structure of singly charged molecular ions is shown in the inset. The intensity of the second isotope is larger than a normal isotopic distribution (see inset). This indicates the presence of molecular radical  $[M+2H]^+*$  cations produced via the electron transfer from electronically excited argon atoms. The second ion is a radical  $[M+2H-NH_3]^+*$  (see inset), since its mass is 1 Da larger than  $[M+H-NH_3]^+$ .

The spectrum of the T18 peptide from an Enolase digest (phosphorylated at tyrosine), fragmented in interaction with metastable argon atoms, is shown in Fig. 4.

Due to the poor mass isolation and the significantly higher intensity of T19 peptide ion signal compared to T18 peptide, the ion signal from the doubly charged T19 phosphorylated peptide and some of its strong fragments are also observed in the presented spectrum. The spectrum of phosphorylated T18 peptide shows c- and z-type ions, along with  $w_{a3}$ ,  $w_{a4}$  and  $y_4$ . The phosphorylation group at tyrosine remains intact during fragmentation, as in the previous case.

The spectrum of a T43 peptide from an Enolase digest (phosphorylated at threonine), fragmented in interaction with metastable argon atoms, is shown in Fig. 5.

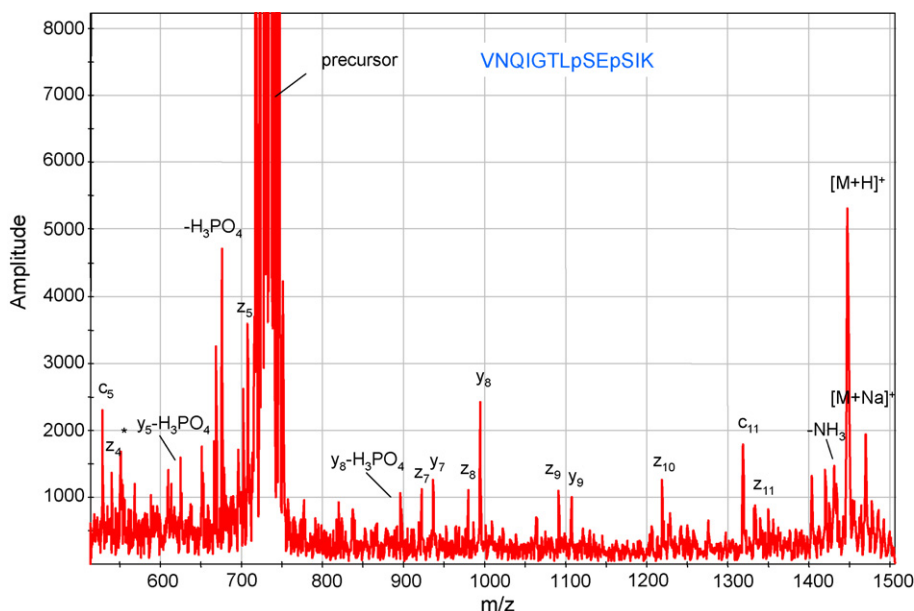


**Fig. 6.** Fragmentation spectrum of doubly charged doubly phosphorylated T43 peptide (VNQIGTLpSEpSIK) from an Enolase digest obtained via interaction with metastable argon atoms (\* denotes unassigned peaks).

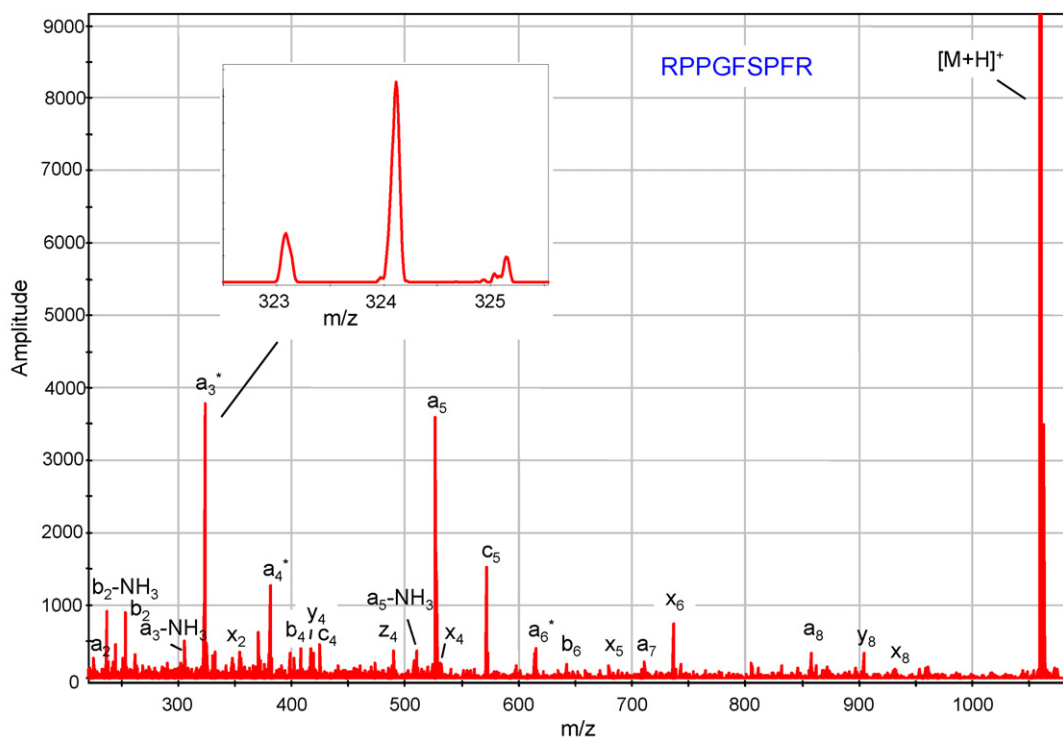


Fig. 7. Fragmentation spectrum of singly charged Bradykinin obtained via interaction with a beam of metastable helium atoms.

The spectrum contains a nearly complete series of c- and z-type fragment ions. The  $w_{a_4}$ ,  $a_4$ ,  $b_4$ ,  $y_4$ ,  $w_{a_5}$ ,  $y_5$ ,  $y_7$ ,  $y_8$ , and  $y_9$  fragment ions were also recorded. No loss of the phosphate group or phosphoric acid from the molecular ion or fragment ions was observed. A strong doubly charged ion signal appearing at  $m/z$  = 657.8 (which is equal to the  $m/z$  of T43 doubly charged molecular ion minus 27) was not identified. Contrary to the cases of the two pre-

vious phosphorylated peptides, no molecular radical cation was observed.

The spectrum of T43 peptide from an Enolase digest (doubly phosphorylated at two serine residues), fragmented in interaction with metastable argon atoms, is shown in Fig. 6.

Formation of c-, z- and y-type ions is observed for this peptide, albeit of weak intensity. Some loss of phosphoric acid from doubly

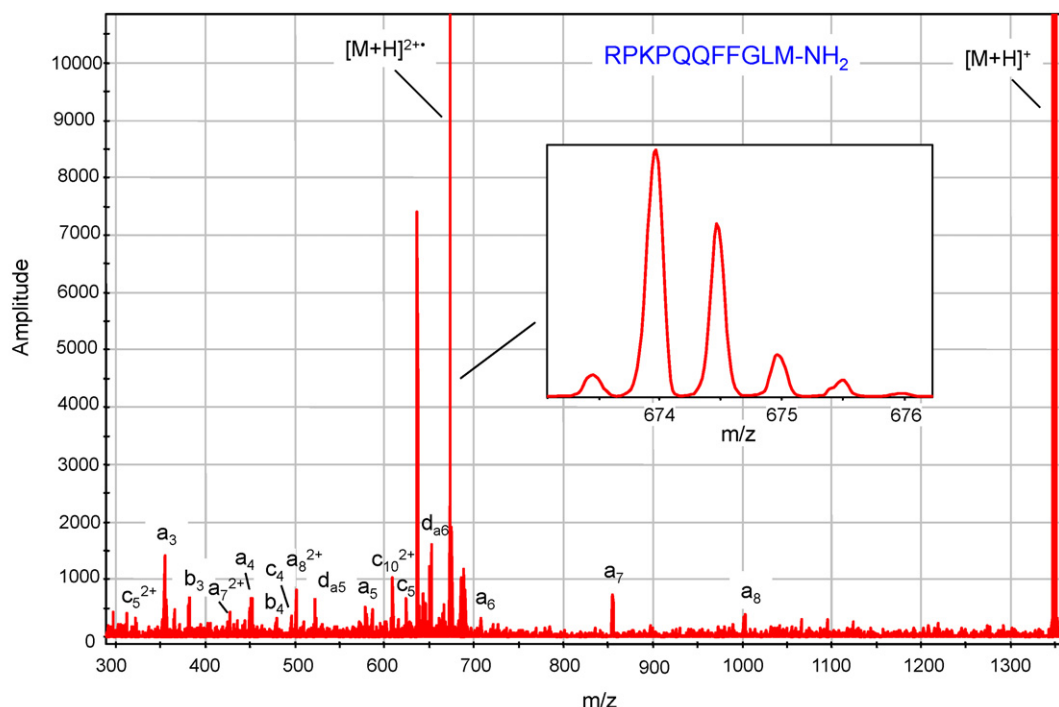


Fig. 8. Fragmentation spectrum of singly charged Substance P obtained via interaction with a beam of metastable helium atoms.

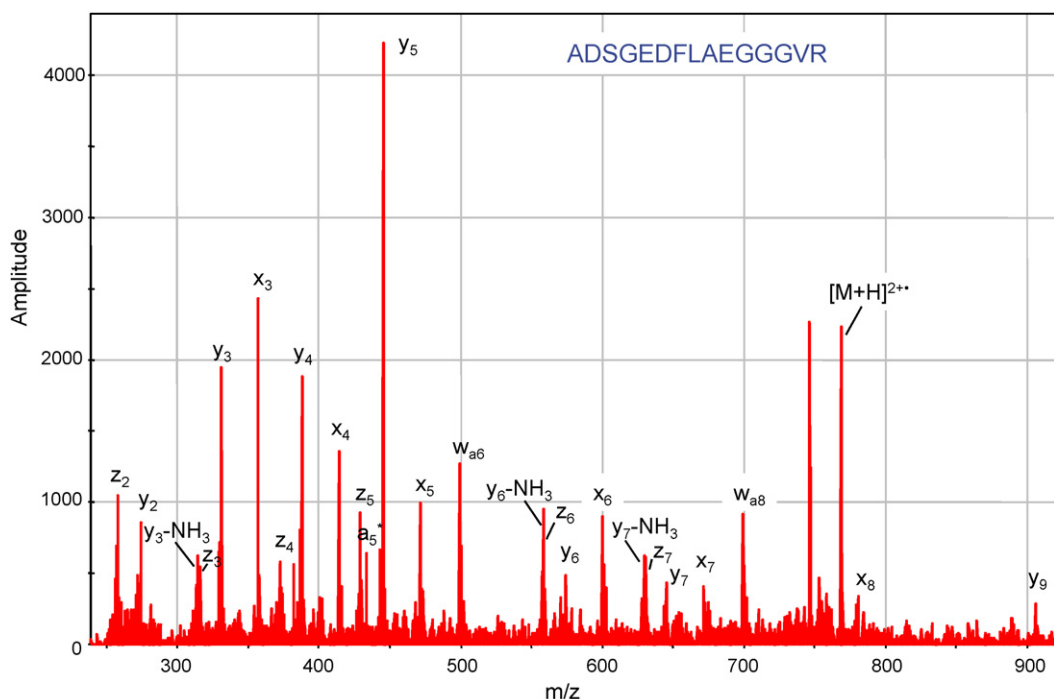


Fig. 9. Fragmentation spectrum of singly charged Fibrinopeptide A obtained via interaction with a beam of metastable helium atoms.

charged molecular ion and y-type fragments is also seen in this spectrum.

As a whole, this data, along with the data presented elsewhere [22], demonstrate the applicability of this new fragmentation technique for studying protein posttranslational modifications.

### 3.3. Fragmentation of singly charged peptides

Singly charged peptides were produced in an electrospray ion source from methanol/water solutions (no acetic acid was added). Mass selection was performed in a resolving quadrupole using Extrel RF/DC power supply, which provides a mass selection window of a few Da. Selected singly charged ions were trapped in the linear ion trap for 100 ms. With the discharge turned off (no electronically excited metastable atoms in the beam crossing the linear trap) only the parent ion was observed. With argon flowing through the discharge source and discharge on, no fragmentation was observed for Bradykinin singly charged molecular ions (data not shown). The picture changed, when helium was used instead of argon (Fig. 7).

The fragmentation mass spectrum is dominated by a series of a-type ions, which result from a backbone cleavage between the  $\alpha$ -carbon and the carbonyl group carbon, with the charge retained on the N-terminal fragment. Some weak x-type ions, which result from the same bond cleavage, but with the charge retained on the C-terminal, are also observed. Several of the a-type ions (denoted by \*) revealed the presence of  $(a+1)^{\bullet}$  radical ion (see inset). It is an odd-electron ion, which forms through a homolytic radical cleavage of the  $\alpha$ -carbon carbonyl-carbon bond. Some y-, b-, c-, and z-type fragments are also observed. The electron transfer from a highly excited metastable state of helium cannot be invoked to explain this fragmentation pattern because it will neutralize the singly charged cation.

Fragmentation spectrum of a singly charged Substance P reveals that fragmentation proceeds via Penning ionization, as shown in Fig. 8.

A strong  $[M+H]^{\bullet 2+}$  ion signal is observed in this spectrum, which is formed via Penning ionization of the  $[M+H]^+$  ions. A strong doubly charged ion at  $m/z=636.8$  (which equals to  $m/z$  of doubly charged radical molecular ion minus 37), was not identified. A nearly complete series of a-type fragment ions is observed, which is consistent with charge retention on the N-terminal (where arginine is located). No radical  $(a+1)^{\bullet}$  ions are recorded, contrary to the fragmentation pattern of a singly charged Bradykinin. A number of d-type fragments, which corresponds to a side-chain loss from a ions, are also observed. Several b- and c-type fragment ions are also present in this spectrum.

The fragmentation spectrum of singly charged Fibrinopeptide A, having a C-terminal arginine residue, is shown in Fig. 9.

In this spectrum a backbone cleavage between the  $\alpha$ -carbon and carbonyl carbon leads to a formation of x-type ions (charge retained on C-terminal). A  $[M+H]^{\bullet 2+}$  ion signal is observed along with a doubly charged ion at  $m/z=746.3$  (which is equal to the  $m/z$  of a doubly charged radical molecular ion minus 22). A nearly complete series of y- and z-type ions are also observed. Several w-type fragment ions, which correspond to a side-chain loss, are also present in the spectrum.

## 4. Conclusions

The application of a new fragmentation method, based on the interaction of peptide cations with electronically excited metastable rare gas atoms, was extended for studying post-translational modifications. Fragmentation of doubly charged phosphorylated peptides from Enolase digest with one phosphorylation group generated mainly c- and z-type peptide fragment ion series. No loss of the phosphate group or phosphoric acid from molecular ion or fragment ions was observed. The formation of a charge-reduced molecular radical cation indicates that the fragmentation mechanism includes the electron transfer from a highly excited metastable state to a peptide cation.

Fragmentation of singly charged peptide cations was performed using electronically excited metastable helium atoms. The formation of  $\alpha$ - or  $\chi$ -type fragment ions, depending on the location of arginine residue in peptide sequence, was observed. Several fragment ions corresponding to a side-chain loss were also observed. The fragmentation mechanism in this case involves Penning ionization of the peptide molecular cation. This feature provides an advantage over ECD/ETD fragmentation techniques, which are not applicable for fragmentation of singly charged peptide cations.

### Acknowledgments

The authors gratefully acknowledge Dr. Peter O'Connor for helpful discussions and the National Institutes of Health for their financial support (SBIR grant 2R44RR022926-02).

### References

- [1] R. Aebersold, M. Mann, *Nature* 422 (2003) 198.
- [2] J.M. Wells, S.A. McLuckey, *Methods Enzymol.* 402 (2005) 142.
- [3] R.J. Simpson, L.M. Connolly, J.S. Eddes, J.J. Pereira, R.L. Moritz, G.E. Reid, *Electrophoresis* 21 (2000) 1707.
- [4] R.A. Zubarev, N.L. Kelleher, F.W. McLafferty, *J. Am. Chem. Soc.* 120 (1998) 3265.
- [5] R.A. Zubarev, N.A. Kruger, E.K. Fridriksson, M.A. Lewis, D.M. Horn, B.K. Carpenter, F.W. McLafferty, *J. Am. Chem. Soc.* 121 (1999) 2857.
- [6] R.A. Zubarev, D.M. Horn, E.K. Fridriksson, N.L. Kelleher, N.A. Kruger, M.A. Lewis, B.K. Carpenter, F.W. McLafferty, *Anal. Chem.* 72 (2000) 563.
- [7] R.A. Zubarev, *Mass Spectrom. Rev.* 22 (2003) 57.
- [8] T. Baba, Y. Hashimoto, H. Hasegawa, A. Hirabayashi, I. Waki, *Anal. Chem.* 76 (2004) 4263.
- [9] O.A. Silivra, F. Kjeldsen, I.A. Ivonin, R.A. Zubarev, *J. Am. Soc. Mass Spectrom.* 16 (2005) 22.
- [10] J.E.P. Syka, J.J. Coon, M.J. Schroeder, J. Shabanowitz, D.F. Hunt, *Proc. Natl. Acad. Sci. U.S.A.* 101 (2004) 9528.
- [11] J.J. Coon, J.E.P. Syka, J.C. Schwartz, J. Shabanowitz, D.F. Hunt, *Int. J. Mass Spectrom.* 236 (2004) 33.
- [12] P.A. Chrisman, S.J. Pitteri, J.M. Hogan, S.A. McLuckey, *J. Am. Soc. Mass Spectrom.* 16 (2005) 1020.
- [13] S.J. Pitteri, P.A. Chrisman, J.M. Hogan, S.A. McLuckey, *Anal. Chem.* 77 (2005) 1831.
- [14] S.J. Pitteri, P.A. Chrisman, S.A. McLuckey, *Anal. Chem.* 77 (77) (2005) 5662.
- [15] A.S. Misharin, O.A. Silivra, F. Kjeldsen, R.A. Zubarev, *Rapid Commun. Mass Spectrom.* 19 (2005) 2163.
- [16] V.D. Berkout, *Anal. Chem.* 78 (2006) 3055.
- [17] P.B. O'Connor, C.E. Costello, W.E. Earle, *J. Am. Soc. Mass Spectrom.* 13 (2002) 1370.
- [18] A.F. Dodonov, I.V. Chernushevich, V.V. Laiko, in: R.J. Cotter (Ed.), *Time-of-flight Mass Spectrometry*, ACS, Washington, DC, 1994, p. 108.
- [19] B.A. Mamyrin, V.I. Karataev, D.V. Shmikk, V.A. Zagulin, *Sov. Phys. JETP* 37 (1973) 45.
- [20] I.V. Chernushevich, A.V. Loboda, B.A. Thomson, *J. Mass Spectrom.* 36 (2001) 849.
- [21] NIST Chemistry WebBook, <http://webbook.nist.gov/chemistry/>.
- [22] V.D. Berkout, *Proceedings of the 54th ASMS Conference on Mass Spectrometry and Allied Topics*, Seattle, WA, 2006.